Prescription for Analysis

⟨author's list goes here⟩

March 18, 2008

Abstract

The goal of this document is to provide detailed directions for the data analysis for E02-013. This experiment is the determination of the electric Sachs form factor of the neutron (G_E^n) from the double polarized asymmetry. The focus of the analysis is to properly determine asymmetry from the reaction $^3\overrightarrow{He}(\vec{e}, e'n)$. This requires an understanding of our polarized target, our electron detector, and our neutron detector. Furthermore, it requires an understanding of the other processes that could be recorded through our detectors.

Contents

1 Introduction

The goal of the analysis to extract values for the Sachs form factor, G_E^n. This will be accomplished by first identifying quasi-elastic electron-neutron scattered events, then forming an asymmetry using the beam electron helicity, then extracting the physics asymmetry, and finally measuring G_E^n by using our physics asymmetry and our kinematic factors. Once the quasi-elastic neutron events are determined, the following equations move the analysis from the counts to the correct physics asymmetry.

$$A_{exp} = \frac{N_+ - N_-}{N_+ + N_-}$$

$$A_{exp} = P_e \cdot P_n \cdot D_{N_2} \cdot D_{background} \cdot A_{phys}, \tag{1}$$

where $N_{+(-)}$ is the number of neutron events with the beam helicity positive(negative), P_e is the beam polarization, P_n is the target polarization, D_{N_2} is a dilution factor due to nitrogen in the cell, $D_{background}$ is the dilution due to background (including proton/neutron conversion), and A_{phys} is used to extract G_E^n. Equation 1 assumes that the background itself does not have an asymmetry. A detailed description of the background asymmetry study can be found in section 6.3.

The next four sections of the introduction will outline how these variables are determined. The final section of the introduction will outline how G_E^n is extracted from A_{phys}. The overall document has the same structure as the introduction.

1.1 Electron Beam

The reaction is started off by the CEBAF electron beam. We need to know the polarization degree, direction, energy, and position of the beam. The polarization degree of the electron beam is used to extract the physics asymmetry from the experimental asymmetry. The helicity and position are recorded for every event. The polarization was measured using Mott, Møller, and Compton polarimeters. The energy was obtained by the ARC measurement of beam deflection through a known magnetic field. The current was measured by the beam current monitors (BCM), and the information is used to correct for false asymmetries due to helicity correlated current asymmetries. Beam halos are particularly important for the present experiment, due to the significant difference (1000 times) in density between the gas of the target and the solid glass walls containing the gas. Operation of the Compton polarimeter provides some monitor of the overall size of this halo. However, the beam must be rastered to prevent damage to the glass cell. Rastering enhances effects due to a beam halo at the extreme position of the beam, even if the inherent size of the halo is small. The enhancement due to rastering allows monitoring of the glass cell scraping.

1.2 Target

For the purposes of analysis, there are several parameters that are required from the target. The primary parameter is the degree of polarization of the target. Like the beam helicity and polarization, the target polarization is a multiplicitive factor relating the experimental asymmetry to the physics asymmetry. Second, the analysis requires precise knowledge of the direction of polarization. The ratio of form factors enters into the equation of the asymmetry weighted by the direction of polarization. The direction was measured by a new compass system developed for E02-013. Energizing the large dipole spectrometer used in the electron arm did effect the direction of the magnetic field. The effect was significant, and was taken into account.

Electron scattering from a variety of targets – hydrogen, carbon, beryllium oxide, and nitrogen – provide information on the electron and hadron optics, the particle identification efficiency and target dilution factors (*e.g.* dilution from nitrogen and from the glass walls of the cell). Additional background can arise from the passage of particles through the materials used in the construction of the target (*e.g.* the glass of the target cell, the ceramic of the target ladder, and the metal of the holding field box). These were carefully measured and will be used as the inputs into a Monte Carlo simulation of the experiment.

The electron beam is deflected slightly by the magnetic fields. This deflection can be taken into account quite easily by a thorough mapping of the magnetic field.

1.3 Electron Arm

The electron arm provides tracking information as well as particle identification and timing. The relevant parameters for determining events in the reaction $^3\overrightarrow{He}(\vec{e},e'n)$ are the momentum of the electron, the angles with respect to the beam-line, and the vertex position along the target. The likelihood that a particle is an electron or some other particle can be determined *via* the preshower and shower calorimeter. Timing information extracted from the electron arm allows us to determine the correct electron beam bunch, which is required for proper neutron arm time of flight analysis. The magnet excitation was fixed throughout the experiment at 710A, which corresponded to a magnetic field of 1.4T. The central angle of the detector was changed one time during the experiment. The central angle of the detector package was surveyed by two independent techniques.

1.4 Neutron Arm

The final piece of equipment required to measure the exclusive reaction is the neutron detector, a large time-of-flight spectrometer. In addition to time-of-flight information, this detector determines the in-plane and out-of-plane scattered angles. Measuring the proper exclusive reaction requires particle identification of the scattered hadron. Veto counters detect if a hadron is charged or not. This is one part of determining if the captured hadron left the target as a proton or an neutron. The characteristics of the more refined particle identification are obtained from measurements on targets with different proton to neutron ratios, Monte Carlo simulations, comparisons with test run data(so-called N20, taken after experiment E01-015), and production run data.

1.5 Analysis

The raw data gathered from the systems above are combined to produce the variables that we need to perform the analysis. First, quasi-elastic neutron events must be identified. But, any sample of these events have contamination from inelastic events which have a different asymmetry and must be taken into account. Identifying this asymmetry requires knowing the direction and magnitude of $\vec{q}$, as well as Q^2 and W. The selection of quasi-free hadrons requires selecting events with small missing parallel and perpendicular momenta. Once the events are selected and the final physics asymmetry is obtained, the value of G_E^n is extracted from the asymmetry[1]:

$$\begin{aligned} A_{phys} &= -\Lambda \cdot \frac{2\sqrt{\tau(\tau+1)}\tan(\theta/2)\sin\theta^* \cos\phi^*}{\Lambda^2 + (\tau + 2\tau(1+\tau)\tan^2(\theta/2))} \\ &\quad - \frac{2\tau\sqrt{1+\tau+(1+\tau)^2\tan^2(\theta/2)}\tan(\theta/2)\cos\theta^*}{\Lambda^2 + (\tau + 2\tau(1+\tau)\tan^2(\theta/2))}, \end{aligned} \tag{2}$$

where $\Lambda = G_E^n/G_M^n$, $\tau = Q^2/4m_N$, θ is the electron scattering angle, θ^* and ϕ^* are the out-of-plane and in-plane momentum transfer angles with respect to the target polarization. Therefore, we must properly understand the scattered electron angle, and the neutron angle with respect to the polarization angle.

In addition to these variables, which describe an ideal, background-free picture, we must account for the background. Data were taken with a variety of targets in an attempt to measure this background. Production data can also be used to to approximate the background. In addition, Monte Carlo methods are employed to approximate, and effectively separate, this background from our data.

[1] This expression is for the asymmetry in the plane wave impulse approximation, corrections due to final state interactions and finite momentum will be applied

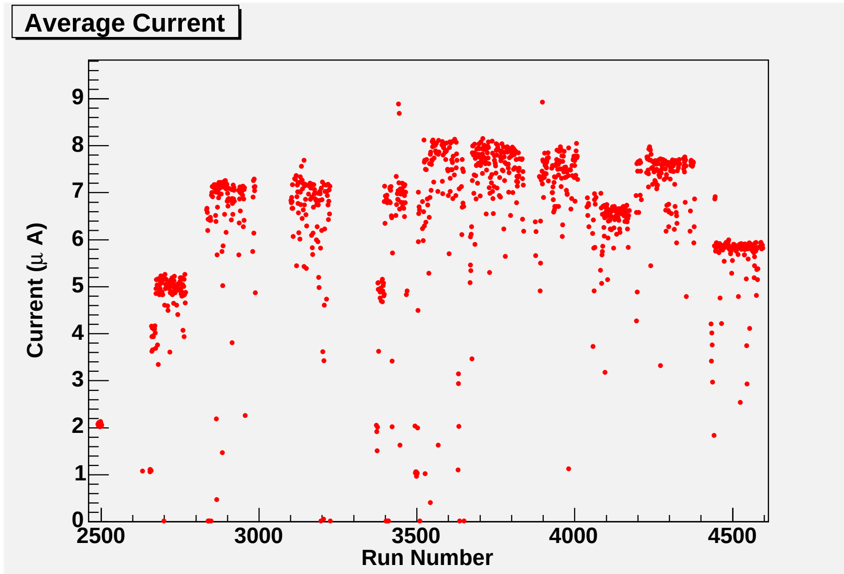

Figure 1: **Average Current Per Run.** The average current as determined by BCM_x3 plotted against the run.

2 Electron Beam

E02-013 used the CEBAF high polarization beam.

The current current used for each run can be seen in Fig. 1, and the accumlated charge per run can be seen in Fig. 2

2.1 Beam Helicity

Properly forming the asymmetry required precise knowledge of the beam helicity. E02-013 used the delayed timing mode which was also used by the parity violating asymmetry experiment G0.

The helicity signal takes a quad structure: +−+, or -++-. Each helicity cycle is 33.3 ms. Each cycle is blind helicity for 0.5ms. This time is necessary for the Pockel cell change, and results in 1.5% of the events having an unknown helicity (denoted as helicity = 0).

A detailed description of the helicity decoding can be found on the E02-013 wiki:
`http://hallaweb.jlab.org/experiment/E02-013/wiki/tiki-index.php?page=Helicity`

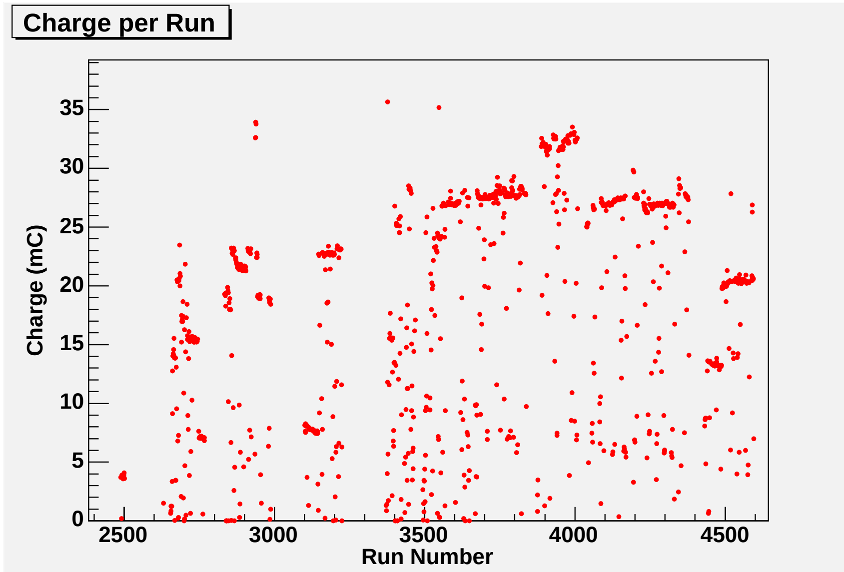

Figure 2: **Accumulated Charge Per Run.** Estimated charge per run plotted against the run.

2.2 Beam Position and Raster

Two beam position monitors (BPM) provide information about the location of the beam within the beamline. These monitors are located 2.215m and 7.517m before the target. These would be sufficient for an unrastered electron beam. However, it is necessary to raster the beam to prevent damage to our target cell, which is made of glass.

The raster is acheived by applying quickly changing magnetic fields to slightly change the direction of the beam. Raster sizes of 2mm x 2mm at the target are typical, and the raster dipoles are located 23m before the target. The raster is created by a triangular waveform applied to two air-core dipole magnets. The result is a uniform rectangular distribution, as seen in Fig. 3.

Because the raster is fast and there is a significant delay between and event and the readout from the BPMs, the BPMs cannot be used to precisely measure the beam when the raster is on. However, the precise vertex of the event can be determined by combining information from the raster current, the BPMs, and spectrometer data taken on optics foils.

The BPMs themselves need to be calibrated against an absolute measure

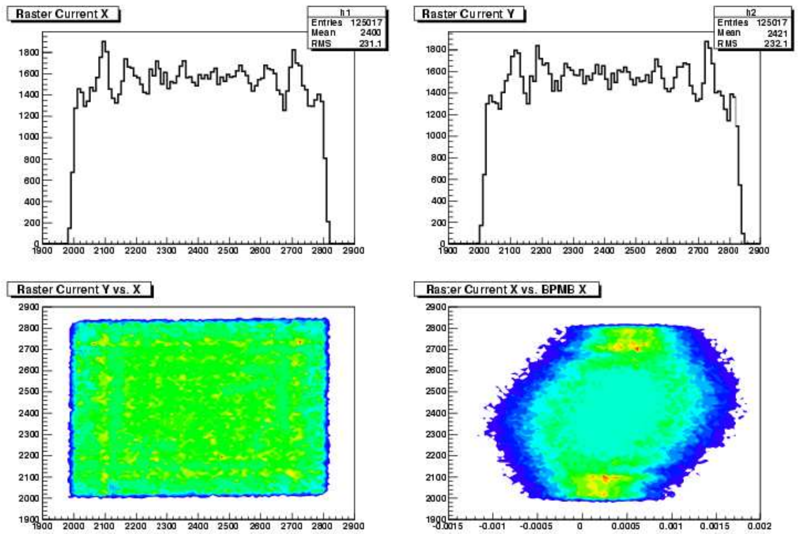

Figure 3: **Raster Currents.** The raster x and y currents as well as the x vs. y and bpm are shown for Kin. 3 optics run #3356.

of the beam position. This is done by a a HARP measurement. HARP measurements are invasive measurements in which a sensing wire is moved into the beamline to determine the location of the beam.

This analysis was performed by Brandon Craver. A document detailing his analysis can be found in the appendix. In addition, the document details the calibration of the BPMs by the HARP measurements.

2.3 Beam Polarization

Eugene Chudakov has studied the polarization of the beam *via* Møller scattering. This technique is based on the cross section of Møller scattering ($\vec{e^-} + \vec{e^-} \rightarrow e^- + e^-$). This cross section depends of the beam and target polarizations.

In practice, the Møller polarimeter consists of a a thin magentically saturated ferromagnetic foil. This results in an average electron polarization of approximately 8%. The foil can be tilted at angles 20-160° to the beam, so that the effective target polarization is $\mathcal{P}^{target} = \mathcal{P}^{foil} \cdot \cos\theta^{target}$. A beam/target asymmetry is formed, and the beam polarization is obtained

Date	Online Pol.(%)	Final Pol.(%)
Feb 28, 2006	88.8 ± 0.2	
Mar 4, 2006	88.2 ± 0.14	
Mar 9, 2006	86.5 ± 0.15	
Mar 25, 2006	82.2 ± 3	
May 10, 2006	$\approx 85\%$	

Table 1: **Møller Measurements.** Beam polarization measurements obtained through Møller scattering.

by:

$$\mathcal{P}_Z^{beam} = \frac{N_+ - N_-}{N_+ + N_-} \cdot \frac{1}{\mathcal{P}^{foil} \cdot \cos\theta^{target} \cdot \langle A_{ZZ} \rangle}, \tag{3}$$

where $\langle A_{ZZ} \rangle$ is the average analysing power, which depends sole on the center of mass angle. This value was obtained from a Monte Carlo calculation of the spectrometer acceptance.

The results can be found in Table 1. The Møller measurements are invasive. They require dedicated beam time, and no production data can be takem.

Additionally, the Hall A Compton polarimeter was used for this experiment. The Compton polarimeter is a non-invasive measurement, and polarization measurements can be taken simultaneous to the polarization measurements. In this measurement, a polarized photon beam scatters from the polarized electron beam. This produces an asymmetry that is related to the beam and target polarization. The equation for the electron polarization is:

$$P_e = \frac{A_e xp}{P_\gamma A_{th}}, \tag{4}$$

where P_e and P_γ are the electron and photon beam polarizations, respectively. A_{th} is the theoretical asymmetry which is the difference over the sum of the cross section, and A_{exp} is the measured asymmetry.

To measure the Compton asymmetry, the electron beam is diverted through a chicane by 4 dipole magnets. In the chicane, the beam intersects an optical cavity, where it interacts with a polarized laser. The backscattered photons

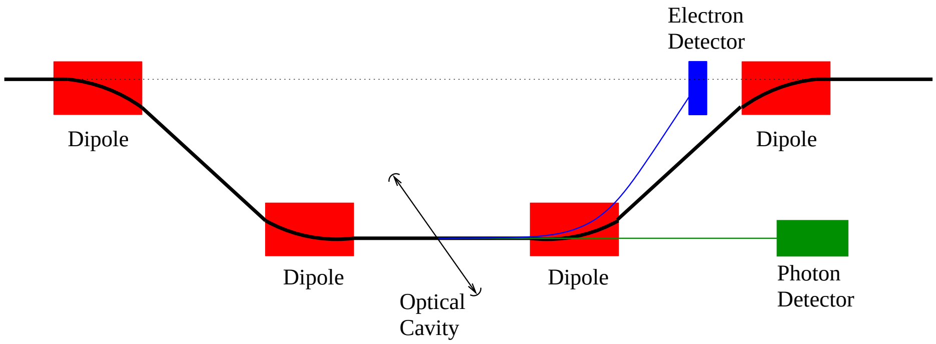

Figure 4: **Compton Chicane.** A schematic of the compton chicane, which allows the electron beam to interact with polarized photon beam and collect both the scattered photon and the scattered electron.

are detected by the photon detector, and the electron beam is directed from the photon detector by the chicane dipoles. Since the scattered electrons lose energy due to their interaction, the scattered electrons can be detected separately to reduce background. A schematic can be seen in Fig. 4

The results of the Compton polarization measurements have been plotted against time in Figure 5

2.4 Beam Energy

Information on the beam energy is primarily the Tieffenbach energy, which is a calculation based on the ARC energy measurement. The ARC energy method measured the deflection of the beam through a magnetic field with a measured field integral.

3 Target

In order to have a double polarized reaction we must have a polarized target in addition to a polarized beam. The ideal target would be high luminosity polarized neutron target. However, polarized neutron targets of sufficient luminosity do not exist.

In place of this ideal, non-existent target, this experiment used a polarized ^{3}He target. Polarized ^{3}He targets have successfully served as substitutes for

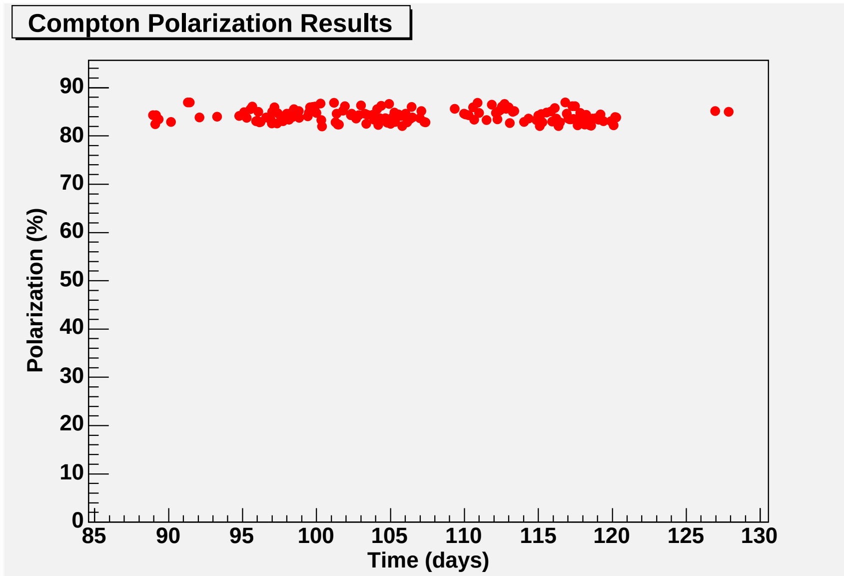

Figure 5: **Compton Measurements.** The results of the Compton polarimeter per day.

Kin.	E (GeV)	Dates	Runs
comm.	3.74	Feb 6 - Feb 22	1483 - 2067
1	1.52	Feb 22 - March 9	2068 - 2784
2a	2.64	March 10 - March 21	2785 - 3333
3	3.29	March 21 - April 17	3334 - 4016
2b	2.64	April 17 - April 24	4017 - 4188
3	3.29	April 24 - May 5	4189 - 4402
4	2.08	May 5 - May 10	4403 - 4656

Table 2: **Kinematics and Beam Energies.** The beam energies for the various kinematic points, as well as the corresponding dates and run numbers are listed.

free-neutron targets in a variety of electron scattering experiments both at Jefferson Lab and at other labs throughout the world. Due to Pauli exclusion principle for the protons in the ground state, nearly 90% of the spin of the polarized ^{3}He nucleus is carried by the neutron. In addition to the small fraction of the spin carried by the proton, polarized ^{3}He targets present additional dilutions to the asymmetry measurement due to the composition of the target.

The first dilution arises from the nucleus itself. A ^{3}He nucleus contains two protons and one neutron. Final state interactions lead to a change in asymmetry, which is under calculation by experts in the field. Quasi-elastic scattering from protons in ^{3} is 5 times more likely than scattering from the neutron. A veto counter is used to determine the charge of the particle as it is detected. However, due to the possible interactions along the path that the particle must take to get from the target to the detector, a conversion from a neutral to charged particle may occur. The details of how this is accomplished can be found in the section on the dilution in the analysis section. The input for that determination is data collected from different solid targets and reference cells.

The second dilution is an artifact of the method used to polarize our ^{3}He target. This target uses the method of spin-exchange optical pumping (SEOP), where circularly polarized laser light is used to polarize an alkali vapor. Atomically polarized vapor spin-exchanges with the ^{3}He nucleus *via* a hyperfine-like interaction. In this process, unpolarized light can be produced that depolarizes the alkali metal. However, the addition of a small quantity of nitrogen quenches the production of unpolarized light, and allows higher polarization.

For E02-013, the target ladder contained: the polarized target, a clear path to the beam dump, a solid target ladder consisting of 6 carbon foils and a BeO foil, and a reference cell that could be evacuated, or filled with different pressures of hydrogen, nitrogen, or unpolarized ^{3}He. The vertical position of the ladder was controlled by a precise step-motor (of XXXX steps per cm).

3.1 Polarization Degree

The results of the target polarization plotted versus productions runs can be found in Fig. 6

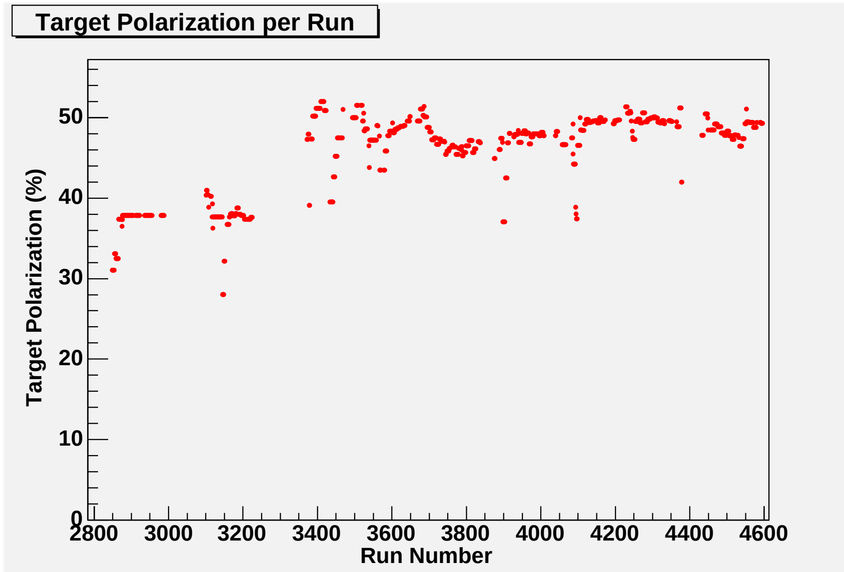

Figure 6: **Target Polarization.** Target polarization plotted versus run number.

3.2 Direction of Magnetic Field

Extracting the proper ratio $\Lambda = G_E^n/G_M^n$ requires precise knowledge of the direction of the polarization. This can be clearly seen in the cosine dependence of θ^* in Eq. 2. A Monte Carlo simulation was performed and the error on G_E^n due to the uncertainty on θ^* was calculated to be as high as 1.6%/mrad, for the $Q^2 = 3.46(\mathrm{GeV}/c)^2$ point. Therefore, the angle of polarization must be known to better than 2mrad to keep the contribution to the uncertainty on G_E^n small.

To reach this required precision, a special compass was designed and built. The compass consists of a permanent magnet on a frictionless air bearing. The airflow required for this bearing did produce a rotation, which was measured and taken into account. The magnetization axis and geometrical axis of the magnet were not coincident, but a rotation of the magnet allowed this effect to be removed from the final measurement.

The direction that the compass pointed in was determined by the using a laser pointer. The laser pointer was fixed in position, and shone on a compass attached to the permanent magnet needle. The reproducability of

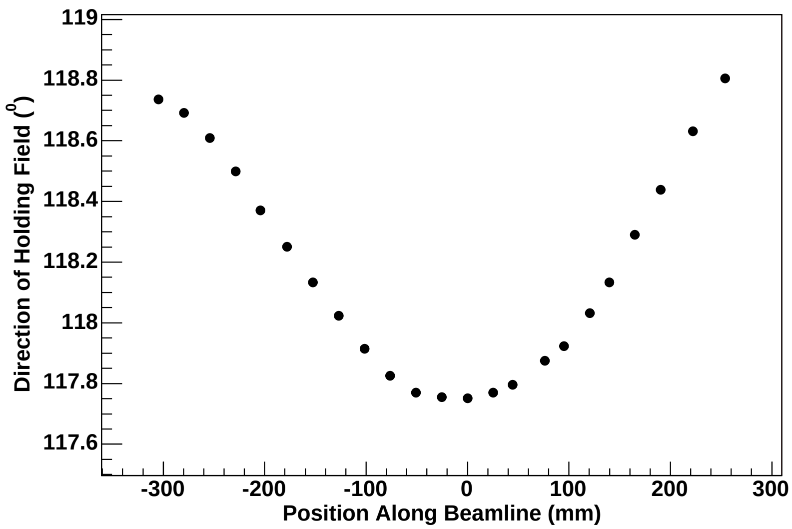

Figure 7: **Magnetic Field Direction.** The magnetic field is plotted as a function of the position along the beamline.

the laser pointer position was accomplised by first shining the light on a fixed reference mirror (figures 13 and 14 from Nelyubin's document). The light was reflected onto a screen. The deflection of the light (with a total pathlength of approximately 6 meters) allowed the magnetic field direction to be determined within 2mrad. These measurements were repeated by moving the compass along the beamline. In addition, vertical spacers were added and removed. In this way, the field direction along the entire length of the cell was mapped, and contributions from the field above and below the beamline were calculated.

The results can be found in Table 3, and plotted in Fig. 7. Along the length of the cell the field direction varies between 118.438° and 117.751°. The minimum occurs at the center of the target cell.

3.3 Nitrogen Contamination

The addition of a small quantity of nitrogen gas to the target cell supresses a specific type of depolarization. However, the prescence of nitrogen also creates a dilution to the asymmetry (represented by the variable D_{N_2} in Eq.

Z (mm)	$\Theta_{hf}(^\circ)$
-304.8	118.737
-279.4	118.692
-254.0	118.609
-228.6	118.499
-203.3	118.371
-177.8	118.251
-152.4	118.133
-127.0	118.023
-101.6	117.914
-76.2	117.826
-50.8	117.770
-25.4	117.755
0.0	117.751
25.4	117.770
44.4	117.796
76.2	117.875
95.2	117.923
120.6	118.032
139.7	118.133
165.1	118.290
190.5	118.438
222.2	118.631
254.0	118.805

Table 3: **Table of polarization direction.** The direction of the magnetic field as measured by the compass designed and built for E02-013.

1). This dilution factor can be obtained by analyzing data collected from the reference cell filled with different pressures of nitrogen.

In essence the dilution factor is determined by comparing the yields in the detectors from the reference cell and the polarized cell.

$$D = 1 - \frac{\rho_{targ}(N_2)}{\rho_{ref}(N_2)} \frac{Y^{(N_2)}}{Y^{(N_2+{}^3He)}}, \tag{5}$$

where $\rho_{ref}(N_2)$ is the density of nitrogen in the reference cell, $\rho_{targ}(N_2)$ is the density of nitrogen in the target cell (a fraction of the total target density), and Y is the yeild.

These yields are the total number of events, after appropriate cuts have been applied, and normalized with charge, livetime, and detector efficiencies. They can be expressed as:

$$Y = \frac{N_{cuts}}{Q \cdot LT \cdot \epsilon \cdot \kappa}, \tag{6}$$

where Q is the accumilated charge, LT is the livetime (combined electronic and computer), ϵ is the combined detector efficiencies, κ is the one track correction factor and N_{cuts} is the number of events after all cuts are applied. These cuts are determined by the ^{3}He analysis.

The one-track correction factor is applied because this is a coincidence experiment. As a coincidence experiment, both electron and neutron arm parameters were included in the analysis. However, the neutron arm detected all events from the multi-track events and the electron arm rejected all but the one-track events.

The correction factor is determined to be

$$\kappa = \frac{\text{number of one track events accepted}}{\text{total number of events for all tracks}}. \tag{7}$$

This need only be determined from the electron arm, as the neutron arm did not skip multi-track events. For production data, $\kappa = 0.498 \pm 0.002$, for nitrogen data 0.542 ± 0.002. The detector efficiencies, ϵ are assumed to be the same for both reference cell and target cell running, so they do not need to be determined explicitly to make

The nitrogen dilution factor must be determined for each kinematic as it is dependent on the $N_2(e, e'n)$ cross section. It is also dependent on the cuts on perpendicular and parallel missing momenta, as the nuclear effects for ^3He and N_2 are different. For kinematic 4, using momentum cuts: $|p_\parallel| <$

Kinematic	$p_{\parallel}$ (MeV/c)	$p_{\perp}$ (MeV/c)	D_{N_2}
1			??
2			??
3	400	150	??
4	250	150	0.955

Table 4: **Nitrogen Dilution for Different Kinematics.** The nitrogen dilution factor varies by Q^2 and by the cuts on missing momentum.

250MeV/c and $|p_{\perp}| < 150$ MeV/c, $D_{N_2} = 0.955 \pm 0.02$. Results for other kinematics can been seen in Table 4.

3.4 Reference Cell

In order to determine the nitrogen dilution, as well as the neutron arm optics and timing, a reference cell was used. The reference cell a glass cell identical to the polarized cell's target chamber. A gas handling system is connected to the inlet of the cell. The cell can then be evacuated and filled with different gasses.

The reference cell is made to the same specifications as the polarized cell. However, the cells are handblown, so some variation will occur. Variations in thickness are measured by the same laser interferomentry technique as is used to characterize the polarized cell.

From the point of view of analysis, the main difference between the polarized cell and the reference cell is in the mounting of the cell to the target ladder. The polarized cell is glued in place, while the reference cell is mounted by it's valve stem. This valve stem is threaded and the fitting has the possibility of rotation. The effect of this possible rotation can be determined by means of the same raster check as used for the polarized cell. In fact, a different set of beam location parameters was used for the reference cell and the polarized cell.

3.5 Solid Targets

A description of the solid targets, with a table of locations and thicknesses should go here. A **brief** description of the BigBite optics calibration can be included.

3.6 Collimators

4 Electron Arm

The electron arm consists of a large non-focusing dipole (called BigBite) and a set of detectors. The set of detectors consists of three multiple wire drift chambers, a calorimeter (consisting of a pre-shower and a shower counter), and a thin scintillator trigger plane.

The detector is called BigBite because it has a large momentum and spatial acceptance. For the configuration used for E02-013, the acceptance was 76 msr over the 40cm length of the target. Even with the larger momentum acceptance, a momentum resolution of 1-2% was acheived. The maximum field used in the experiment was 1.4T.

The drift chamber consist of three separate horizontal drift chambers spaced approximately 35cm apart. The drift chambers are the first set of detectors after the magnet and are the highest spatial resolution detectors in the full set. Tracking information was derived primarily from these drift chambers.

From the Wiki (to be re-written): "To achieve the ability to resolve points in three dimensions, three different types of planes are used, which we call U, X, and V. All three plane types reside in a plane of constant z (w/r/t the detector co-ordinates). X wires run parallel to the Y axis and U and V wires are 30° to that axis (see figure). In each plane, the sense wires are spaced 1cm apart, with a field shaping wire in between each pair. Planes of the same type, when next to each other, are staggered 0.5cm relative to one another. The chambers are filled with a 50% argon-50% ethane gas mixture kept at slightly above atmospheric pressure.

The sense wires are triggered as a charged particle ionizes the gas when it passes through the chamber. If the wires are then put at some potential difference, the free floating charges drift towards the wires and generate an electrical signal which is then read out by a time-to-digital converter. The amount of time it takes to drift from the track to the wire can then be converted into a distance.

The purpose of the tracking code is to take these times, convert them to a distance, and then use these distances to fit a straight line across several planes"

Much of the electron arm geometry information comes from the data (ask Seamus). However, a detailed survey of the position of the spectrometer

was made by Eugene Chudakov, and can be found at the following website:
`http://hallaweb.jlab.org/experiment/E02-013/surveys.html`

5 Neutron Arm

The Neutron Detector (sometimes called BigHand or NeutronArm) contains two thin veto planes followed by the neutron-detector planes: seven planes of converter material/scintillator. Each veto plane is composed of independent left-and-right scintillators read out on one end, with a total of 48 * 2 = 96 detectors per plane. The active region of the neutron detectors are 5 or 10cm thick scintillator bars read out on both sides, providing a horizontal position as well as precise timing information. The segmentation of the neutron detector planes permits a coarse determination of the neutron's vertical position.

Detection of an event – Need to talk to Jonathon to get the story. Once I have a framework, there is very good information on the wiki.

information for this section can be obtained from Tim Ngo's work, as stored in the GEn website.

6 Analysis

6.1 Raw Asymmetry

6.2 Dilution

As noted in Section 5, the neutron detector identifies hadrons and uses the veto counters to determine if the event was charged or uncharged. This should be sufficient to determine if the particle scattered from the target was a proton or a neutron. However, the particle must travel through materials and may experience a charge conversion before reaching the veto plane. This conversion may occur for both protons and neutrons. The effect of this conversion can be determined through a thorough Monte Carlo analysis of the scattering process. In addition, insight may be gained through the analysis of data collected during the experiment.

The relevant parameter for this discussion is the fraction of particles that are protons or neutrons from the total number of charged or uncharged counts.

$$
\begin{aligned}
f_n &= \frac{N_n^n}{N_n^n + N_p^n} && (8)\\
f_p &= \frac{N_p^c}{N_n^c + N_p^c}, && (9)
\end{aligned}
$$

where $N_{n,p}^{n,c}$ is the number of neutrons or protons detected as neutral or charged. Likewise the total number of observed neutral and charged events can be written in these terms:

$$
\begin{aligned}
N^c &= N_n^c + N_p^c && (10)\\
N^n &= N_n^n + N_p^n && (11)
\end{aligned}
$$

Both charged and uncharged particles are detected by the same detector. Therefore, factors of the target luminosity, beam intensity, and angular acceptance are common to all.

$$
\begin{aligned}
N_n^n &\propto (A - Z)\sigma_n \eta_n^n && (12)\\
N_p^c &\propto Z\sigma_p \eta_p^c, && (13)
\end{aligned}
$$

where A(Z) is the atomic mass(number) of the target, $\eta_{n,p}^{n,c}$ is the overall efficiency of detecting the neutron or proton as a neutral or charges particle. The neutron and proton electron cross sections are $\sigma_{n,p}$.

By rewriting the Eqs. 8 and 9 in terms of these efficiencies and cross sections and dividing numerator and denominator by $\sigma_p \eta_p^c$, the fractions for ^{3}He are written:

$$
\begin{aligned}
f_n^{^3He} &= \frac{\frac{\sigma_n}{\sigma_p}\left(\eta_n^n/\eta_n^c\right)}{\frac{\sigma_n}{\sigma_p}\left(\eta_n^n/\eta_n^c\right) + \frac{p}{n}\left(\eta_p^n/\eta_p^c\right)} && (14)\\
f_p^{^3He} &= \frac{\frac{p}{n}}{\frac{\sigma_n}{\sigma_p}\left(\eta_n^c/\eta_p^c\right) + \frac{p}{n}}, && (15)
\end{aligned}
$$

where p/n is the ratio of protons to neutrons in the ^{3}He nucleus.

Ratios of the number of particles detected as a charged or uncharged hadron can be written as

$$R_{n/c} = \frac{N^n}{N^c} = \frac{(A-Z)\sigma_n\eta_n^n + Z\sigma_p\eta_p^n}{(A-Z)\sigma_n\eta_n^c + Z\sigma_p\eta_p^c}. \tag{16}$$

During the experimental run, targets of ^{3}He, H_2, N_2, and mixed C/BeO were used. These provide data from targets with different ratios of (A-Z)/Z. It is useful, therefore, to re-write Eq. 16 in terms of this ratio:

$$R_{n/c} = \frac{\frac{(A-Z)}{Z}\frac{\sigma_n}{\sigma_p}\left(\eta_n^n/\eta_p^c\right) + \left(\eta_p^n/\eta_p^c\right)}{\frac{(A-Z)}{Z}\frac{\sigma_n}{\sigma_p}\left(\eta_n^c/\eta_p^c\right) + 1}. \tag{17}$$

This can be used to specify the ratios for relevant to each target.

$$R_{n/c}^{H} = \eta_p^n/\eta_p^c \tag{18}$$

$$R_{n/c}^{N,C,BeO} = \frac{\frac{\sigma_n}{\sigma_p}\left(\eta_n^n/\eta_p^c\right) + \left(\eta_p^n/\eta_p^c\right)}{\frac{\sigma_n}{\sigma_p}\left(\eta_n^c/\eta_p^c\right) + 1} \tag{19}$$

$$R_{n/c}^{^3He} = \frac{\frac{\sigma_n}{\sigma_p}\left(\eta_n^n/\eta_p^c\right) + 2\left(\eta_p^n/\eta_p^c\right)}{\frac{\sigma_n}{\sigma_p}\left(\eta_n^c/\eta_p^c\right) + 2} \tag{20}$$

In terms of the ratios of efficiencies:

$$\frac{\eta_p^n}{\eta_p^c} = R_H \tag{21}$$

$$\frac{\eta_n^n}{\eta_p^c} = \frac{\sigma_p}{\sigma_n}\frac{\left(\frac{p}{n}-1\right)R_N\left(R_{^3He}-R_H\right) - R_H R_N + R_{^3He}R_H}{R_N - R_{^3He}} \tag{22}$$

$$\frac{\eta_n^c}{\eta_p^p} = \frac{\sigma_p}{\sigma_n}\left(\frac{\left(\frac{p}{n}-1\right)\left(R_{^3He}-R_H\right)}{R_N - R_{^3He}} - 1\right) \tag{23}$$

Then Eqs.14 and 15 can be written in terms of these ratios:

$$f_n^{^3He} = \frac{\left(\frac{p}{n}-1\right)R_N(R_{^3He}-R_H) - R_H R_N + R_{^3He}R_H}{\left(\frac{p}{n}-1\right)\left(R_{^3He}-R_H\right) - R_N + R_{^3He}} \tag{24}$$

$$f_p^{^3He} = \frac{\frac{p}{n}(R_N - R_{^3He})}{(\frac{p}{n}-1)(R_{^3He}-R_H) + R_N - R_{^3He}} \tag{25}$$

These fractions have been left in terms of the ratio of the number of protons to the number of neutrons. This ratio is naively 2 for ^{3}He. However, the ratio is a function of initial momentum.

6.3 Background

Include description of the information obtained through the measurements on the empty target and the empty reference cell.

An additional, serious source of background could have come from a scraping of the beam along the glass walls of the cell. The beam must be rastered in order to run on the glass cell of the polarized ^{3}He target. A slight misalignment of the target with respect to the beam could produce electron scattering from the thick walls of the target cell. This scattering might not be seen at low raster currents (corresponding to small deflections of the beam, centered on the target). If there is a marked increase in the detector rate as the raster current increases, this will indicate that there is scraping, and it will tell us how large the raster must be to see the scraping.

This analysis has not been performed, who should perform it?

Also, talk about how background is handled by looking at production data (i.e. the time-of-flight (or $\vec{q}_\perp$ spectrum is shifted so that the proper cuts can be applied to a non-physical region).

6.4 Monte Carlo Simulation

To truly analyze the reaction, a Monte Carlo simulation is required. Such a simulation will simulate three classes of events: $(e, e'n)$, $(e, e'p)$ and random background. The random background is made up of events from the $(e, e'X)$ reaction, as well as accidentals. A model is required for all three processes.

A Monte Carlo will require two classes of inputs. First, it requires physics inputs (described in Section 1.5). Second, it requires detector parameters. Specifically, it requires the resolution and acceptance of the detectors. In addition it requires particle identification from the detectors. This is slightly more sophisticated than the particle detection in the detector analysis. The efficiency of the detectors for different particles is an essential input into a Monte Carlo simulation.

6.5 Physics Analysis